

Properties of high-redshift quasars – I. Evolution of the supermassive black hole to halo mass ratio

J. Stuart B. Wyithe¹★ and T. Padmanabhan²★

¹*School of Physics, University of Melbourne, Parkville, Victoria, Australia*

²*Inter-University Centre for Astronomy and Astrophysics, Pune, India*

Accepted 2005 November 9. Received 2005 November 9; in original form 2005 January 17

ABSTRACT

In the local Universe, the masses of supermassive black holes (SMBHs) appear to correlate with the physical properties of their hosts, including the mass of the dark matter haloes. At higher redshifts, we observe the growth of SMBHs indirectly through the identification of high-redshift quasars. However, information on their hosts is more difficult to obtain. In this paper, we determine the masses of the haloes that host the high-redshift quasars (at $z > 4$) by comparing the rate of growth of quasar density with that predicted by the Press–Schechter mass function. The host mass determined depends on how the ratio between the SMBH and the host halo mass evolves with redshift. Under the assumption that the ratio between the SMBH and the halo mass does not evolve with redshift, we find a host halo mass of $M = 10^{11.7 \pm 0.3} M_{\odot}$. Even if the quasars shine at their Eddington limit, this host mass is significantly smaller than that seen at lower redshifts in the local Universe. Indeed, we find that the null hypothesis, of a constant ratio between the SMBH and the halo mass at all redshifts, can be ruled out at greater than a 5σ level. SMBHs must therefore have contributed a larger fraction to the host mass in the past. This finding is consistent with expectations from models of self-limiting SMBH growth. When we include the redshift evolution of the ratio between the SMBH and the halo mass, we find larger halo masses of $M \sim 10^{12.4 \pm 0.3} M_{\odot}$, in combination with a ratio between the SMBH and the host halo mass that increases with redshift in proportion to $\sim(1+z)^{1.5}$, are required to be consistent with both local and high-redshift observations. We also investigate the restrictions placed on the critical linear overdensity of quasar hosts at their epoch of virialization, and find that it cannot exceed the traditional value of $\delta_c = 1.69$ by more than a factor of 2. Finally, we find that the high-redshift quasars are hosted by fluctuations on scales that have a variance of $\delta M/M = 2\text{--}3$, corresponding to $(3\text{--}4.5)\sigma$ fluctuations in the density field.

Key words: galaxies: formation – cosmology: theory.

1 INTRODUCTION

The Sloan Digital Sky Survey (SDSS) has discovered luminous quasars at redshifts as high as $z \sim 6.4$, i.e. when the Universe was only a billion years old. The supermassive black holes (SMBHs) powering these quasars have been estimated to have a mass of about 10^9 solar masses. However, questions regarding the galaxies that host these high-redshift quasars have remained largely unanswered. To understand the formation and evolution of quasars and the SMBHs that power them, one needs to determine several important physical parameters (such as the quasar lifetime, the ratio of black hole mass to halo mass and the efficiency and rate of accretion during the luminous phase), as well as the evolution of these

parameters with time. Attempts to answer these questions generally consider the quasar luminosity function, as it provides a tracer of the density of quasars with different luminosities as a function of cosmic epoch (e.g. Haehnelt, Natarajan & Rees 1998; Haiman & Loeb 1998; Kauffmann & Haehnelt 2000; Volonteri, Haardt & Madau 2003; Wyithe & Loeb 2003). However, all these analyses are model dependent and implicitly assume either (a) the quasar lifetime and its evolution with redshift and/or (b) the form, normalization and evolution of a relation between the SMBH mass and the characteristic velocity of the host galaxy. The exceptions are studied at low redshift that utilize the quasar two-point correlation function (Haiman & Hui 2001; Martini & Weinberg 2001; Croom et al. 2005). At high redshift, dynamical estimates have been made in a few individual cases (Barkana & Loeb 2003; Bertoldi et al. 2003).

Locally, direct estimates of the SMBH and the host mass can be made through observations of galaxy dynamics. These observations reveal a correlation between the SMBH mass and the characteristic

★E-mail: swyithe@isis.ph.unimelb.edu.au (JSBW); nabhan@iucaa.ernet.in (TP)

velocity of the surrounding stellar spheroid (e.g. Merritt & Ferrarese 2001; Tremaine et al. 2002), and by extension of the host dark matter halo (Ferrarese 2002). These characteristic velocities determine the dynamical mass, so that there are also corresponding correlations between the SMBH and the host mass. Any proposed scenario for the SMBH evolution must reproduce this behaviour, and hence the correlations provide important clues regarding the physics of formation of SMBHs.

However, at higher redshift, objects collapse out of a denser background. The characteristic velocity of a virialized object of a given halo mass is therefore larger if it formed at higher redshift. This raises the question of whether the fundamental correlation is between the SMBH mass and the hosts' characteristic velocity, or between the SMBH mass and the dynamical host mass. Obviously, knowledge of which correlation is fundamental is critical for our understanding of the astrophysics of SMBH evolution. Unfortunately, since these dynamical observations can only be made for relatively nearby galaxies, this question cannot be resolved via direct observation.

Here, within the paradigm of standard concordance cosmology, we show that by associating halo mass with quasar luminosity, the formation rate of luminous quasars in the high-redshift Universe can be used to constrain the mass of the dark matter haloes that host them. We thus provide a framework within which one can attempt to answer the question of whether the host mass or the velocity is the determining factor in the evolution of a SMBH. We believe that this procedure holds significant promise for the future when the observations improve. Our approach differs philosophically from previous semi-analytic studies, which generally hypothesize a model that encapsulates various assumptions for the relevant astrophysics (such as the nature of feedback). These models are then used to generate a quasar luminosity function which may be compared with observations. In this paper, we limit our assumptions to standard linear cosmology, and derive statistical constraints on the parameters of halo mass and lifetime for high-redshift quasars. These constraints have statistical as well as systematic uncertainties. The latter are quantified via the dependence of the results on parameters describing the unmeasured trends of variation of SMBH occupation fraction and quasar lifetime with redshift, and that of SMBH to halo mass ratio with redshift.

The optical quasar luminosity function shows a peak in its evolution at $z \sim 2-3$. At higher redshifts, the quasar population grows with time, and it is natural to relate the rise of the quasar population to the rise of the dark matter halo population (e.g. Haehnelt et al. 1998; Haiman & Loeb 1998; Volonteri et al. 2003; Wyithe & Loeb 2003). However, near a redshift of $z \sim 2-3$, the non-linear mass-scale moves from galaxy mass to group and cluster mass objects. It is thought that the rapid fall in the density of bright quasars below $z \sim 2$ is due to a combination of a dwindling supply of cold gas at late times (Kauffmann & Haehnelt 2000) with an injection of feedback from the quasars into the surrounding intergalactic medium that prevents further gas accretion on to collapsing systems (Scannapieco & Oh 2004). Following the peak of quasar evolution, one can no longer relate the growth of the quasar (or galaxy) population directly to that of the dark matter halo population in any direct or model independent way. For these reasons, we restrict our attention to quasars at redshifts beyond $z \sim 3.7$, where we can relate the evolution in the quasar luminosity function directly to evolution of the Press & Schechter (1974) mass function.

In Section 2, we begin with the null hypothesis that the ratio between the masses of SMBH and the halo does not evolve with redshift. Under this assumption, we find the host mass to be about

$10^{11.7 \pm 0.3} M_{\odot}$. Estimates for SMBH mass powering the luminous SDSS quasars yield $\sim 10^9 M_{\odot}$ assuming output at the Eddington limit (the Eddington limit provides a lower limit on SMBH mass, and hence a lower limit on the mass ratio). The resulting SMBH to halo mass ratio is therefore much larger for the SDSS quasars than for local galaxies. Indeed, the null hypothesis can be rejected at a significance greater than 5σ , i.e. SMBHs in the past contributed a larger fraction of galaxy mass than that of today. This is one main conclusion of the paper. Next, we allow for the SMBH to halo mass ratio to evolve with redshift (Section 2.6). In this general case, we estimate a halo mass for high-redshift quasar hosts, $M \sim 10^{12.4 \pm 0.3}$, and find that the ratio between the SMBH and the host halo mass should increase with redshift as $\sim (1+z)^{1.5}$ in order to be consistent with extrapolation from local observations. Estimates for the high-redshift quasar lifetime are discussed in Section 3. We also investigate variance of the linear power spectrum on the scale of density fluctuations corresponding to the high-redshift quasar hosts in Section 4. Finally, we discuss the implications of the rate of high-redshift quasar density evolution for the value of the critical linear overdensity at host virialization in Section 5. Some concluding discussion is given in Section 6.

Throughout the paper, we adopt the set of cosmological parameters determined by the *Wilkinson Microwave Anisotropy Probe* (WMAP; Spergel et al. 2003), namely mass density parameters of $\Omega_m = 0.27$ in matter, $\Omega_b = 0.044$ in baryons, $\Omega_{\Lambda} = 0.73$ in a cosmological constant and a Hubble constant of $H_0 = 71 \text{ km s}^{-1} \text{ Mpc}^{-1}$. For the primordial power spectrum of density fluctuations, we adopt a power-law slope $n = 1$, and the fitting formula to the exact transfer function of Bardeen et al. (1986). It turns out that our results are most sensitive to the cosmological parameter σ_8 , which is the amplitude of the linearly extrapolated power spectrum on scales of $8 h^{-1} \text{ Mpc}$. We present results for different σ_8 wherever appropriate to illustrate the range of this dependence.

2 EVOLUTION IN QUASAR DENSITY

The Press & Schechter (1974) mass function [with the modification of Sheth & Tormann (2002) that will be adopted throughout our discussion] yields the number density $N[>M(z), z]$ of dark matter haloes above some mass $M(z)$ at redshift z . If luminous quasars reside in a fraction ϵ of such dark matter haloes, then the observed number density of quasars is given by the product of two factors: $N[>M(z), z]$ and $\tau \equiv \epsilon \min\{t_q/H^{-1}(z), 1\}$, where t_q is the (unknown) quasar lifetime and $H^{-1}(z)$ is the Hubble time (see e.g. Efsthathiou & Rees 1998). As a measure of the rate at which luminous quasars appear, we use the logarithmic derivative (B) of $\tau N[>M(z), z]$, defined as

$$B = \frac{d \log \tau}{dz} + \frac{\partial \log N(>M, z)}{\partial z} + \frac{\gamma}{(1+z)} \frac{d \ln N(>M, z)}{d \ln M}. \quad (1)$$

Here, we have assumed that the halo mass varies as $M \propto (1+z)^{\gamma}$ at fixed luminosity M_{1450} . This choice is convenient for our discussion because observations do reveal an exponential decline in the quasar population with redshift suggesting approximate constancy of B . Our analysis, of course, relies on the applicability of the Press–Schechter mass function (as modified by Sheth & Tormann 2002). It has been shown that this analytic formalism provides an excellent description of the halo mass function found from numerical simulations (Jenkins et al. 2001). In particular, if the numerical mass function is expressed in the appropriate variables then it is independent of epoch, which is a defining feature of the Press–Schechter formalism. Evaluation of B using the Press–Schechter mass

function therefore provides an accurate description of the redshift evolution of massive dark matter haloes in a Lambda cold dark matter (Λ CDM) cosmology.

Many modern formulations of model quasar luminosity functions include major galaxy mergers as the trigger for luminous quasar activity (e.g. Kauffmann & Haehnelt 2000; Volonteri et al. 2003; Wyithe & Loeb 2003). An alternative approach to equation (1) could therefore be to replace the quantity $N(>M)$ with an integral over the product of the halo mass function with the number of major mergers per quasar lifetime. This approach would require an additional hypothesis relating quasar activity to major mergers, whereas we prefer to limit ourselves to a single physical hypothesis; that SMBH masses are related to their host dark matter haloes. However, we note that within a merger-driven formulation, the number density of quasars is proportional to the number of major mergers and to the ratio between quasar lifetime and the Hubble time. Broadly speaking, the effect of major mergers can therefore be absorbed within the evolution of τ .

The mass function $N(>M, z)$ leads to a steeper slope B as M is increased. This is illustrated by the grey dot-dashed lines in the left-hand panel of Fig. 1 which shows the evolution of $N(>M, z)$ (arbitrarily normalized at $z = 4.8$) for masses of 10^{10} , 10^{11} , 10^{12} and $10^{13} M_{\odot}$. These curves should be compared with the observed evolution in the density of luminous ($M_{1450} < -26.7$) quasars between redshifts of $z \sim 3.7$ and 6 from the SDSS (Fan et al. 2001a, 2003, 2004), which is also summarized in the same panel. Here, we are assuming that the identification of luminosity M_{1450} with halo mass M does not vary (i.e. $\gamma = 0$). This forms the null hypothesis in this work. The effects of relaxing this assumption are discussed in Section 2.6.

The curves corresponding to 10^{11} and $10^{12} M_{\odot}$ have logarithmic slopes that lie at the extremes of the range allowed by the data. It is therefore clear that if we can measure the exponential slope in the formation of high-redshift quasars, then we can determine the mass of their host dark matter haloes. By using only the logarithmic slope B , we have removed the dependence on the *absolute value* of quasar lifetime. However, B does depend on the form of the redshift *evolution* of τ (and on γ). While ϵ could also change with z due to various effects (dust obscuration, beaming angle, etc.), we expect the dominant additional contribution to B to come from t_q . The z dependence of t_q can be handled by using two physically motivated forms for the evolution – which bracket the reasonable range of possibilities – and can be parametrized by $\tau \propto (1+z)^{\alpha}$ with $0 \lesssim \alpha \lesssim 3/2$. First, if the quasar lifetime is determined by the mass

e-fold time-scale of the SMBHs, then t_q is independent of redshift, $\tau \propto 1/H^{-1}(z)$ and $\alpha \approx 3/2$. Secondly, if the quasar lifetime is determined by the dynamical time-scale at z , then $t_q \approx H^{-1}(z)$ making τ independent of redshift and $\alpha \simeq 0$. [This is also true if $t_q > H^{-1}(z)$.]

2.1 Evolution constraints

The evolution shown in Fig. 1 is well fitted by an exponential decline (Fan et al. 2001a) of the form

$$\Psi(M_{1450} < -26.7, z) \propto 10^{B_{\text{obs}} \times z}. \quad (2)$$

The right-hand panel of Fig. 1 shows the a posteriori differential (grey curves) and cumulative (black curves) probability distributions for the observed exponential slope B_{obs} . These distributions were computed as follows. For each value of B_{obs} , we find the normalization which maximizes the product of probabilities from each redshift bin (assuming Gaussian error bars). This product represents the likelihood for B_{obs} . A flat prior probability for B_{obs} was then assumed, allowing calculation of a posteriori distributions for B_{obs} . Distributions were estimated using (i) the whole data set and two subsets of the data, (ii) data with $z < 5$ and (iii) data with $z > 4.5$. We find that $B_{\text{obs}} \sim -0.49 \pm 0.07$, -0.52 ± 0.15 and -0.53 ± 0.20 describe the evolution within the full data set and two subsets, respectively, showing internal consistency. The best fit is also plotted in the top left-hand panel to guide the eye.

2.2 Mass constraints

From equation (1), there is a one-to-one monotonic correspondence between halo mass M and exponential slope B . The a posteriori probability distributions for host halo mass, M , may therefore be found by noting that

$$\frac{dP}{dM} \propto \left. \frac{dB}{dM} \right|_{B=B_{\text{obs}}} \frac{dP}{dB_{\text{obs}}}, \quad (3)$$

where dB/dM was computed using equation (1) at the central redshift within the luminosity function data. The differential (grey lines) and cumulative (dark lines) a posteriori distributions for M are plotted in the left-hand panel of Fig. 2. If $\alpha = 3/2$ (solid lines), the observed evolution in the density of bright quasars implies host haloes with masses of $10^{11.9 \pm 0.2} M_{\odot}$. If $\alpha = 0$ (dashed lines), then the halo mass estimates and their upper bounds are about a factor of 2 smaller; we get $10^{11.6 \pm 0.2} M_{\odot}$. Thus, under the null hypothesis of a

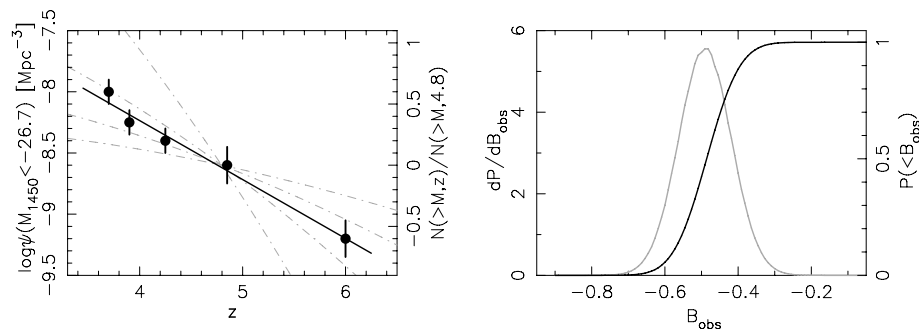


Figure 1. Constraints on the evolution of the density of high-redshift quasars. Left-hand panel: the density of quasars with $M_{1450} < -26.7$ as a function of redshift (Fan et al. 2001a, 2003, 2004). The solid line shows the best-fitting exponential decline $\Psi(< 26.7, z) \propto 10^{B_{\text{obs}} \times z}$ to the full data set, with $B_{\text{obs}} = -0.49$. For comparison, the evolution in the density of haloes (normalized to unity at $z = 4.8$) with masses of 10^{10} , 10^{11} , 10^{12} and $10^{13} M_{\odot}$ are shown by the grey dot-dashed curves in order to decreasing steepness. Right-hand panel: the corresponding a posteriori differential (grey lines; left axis) and cumulative (black lines; right axis) probability distributions for B_{obs} .

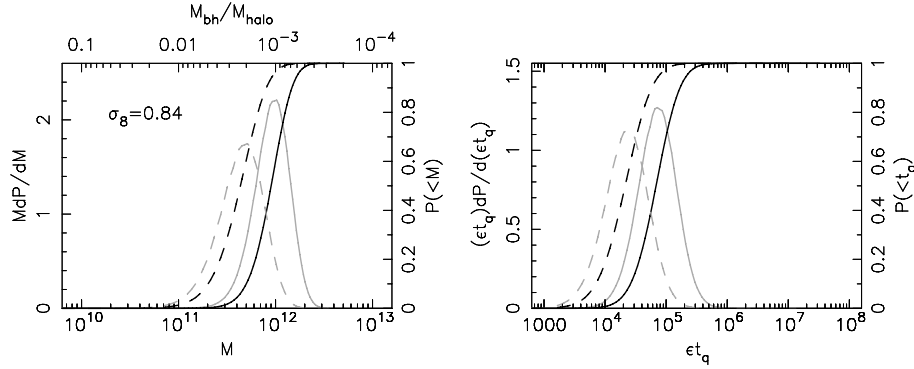


Figure 2. Constraints on the mass of the halo that hosts a high-redshift quasar. Left-hand panel: the a posteriori differential (grey lines) and cumulative (dark lines) probability distributions for M (solid lines $\alpha = 3/2$, dashed lines $\alpha = 0$; $\gamma = 0$). The upper axis shows the corresponding values for fraction of halo mass contributed by a $10^9 M_\odot$ black hole. Right-hand panel: the corresponding differential (grey lines) and cumulative (dark lines) probability distributions for ϵt_q . All curves in this figure were evaluated for $\sigma_8 = 0.84$.

fixed $\gamma = 0$, the exponential slope of the high-redshift quasar luminosity function leads to the determination of masses of haloes that host high-redshift quasars to within a factor of a few. In particular, we stress that the result does not rely on any a priori assumptions about the relation between the quasar luminosity and the SMBH mass, about the relation between the SMBH and the halo mass, or about the halo density profile.

As an aside, we note that an alternative approach to equations (3) and (5) for calculation of dP/dM [and $dP/d(\epsilon t_q)$] would be to choose prior probabilities for M and ϵt_q that are flat in the logarithm, and likelihoods for M and ϵt_q based on the comparison of the corresponding slope with the data. We find that this approach gives nearly identical results to those presented in this paper.

2.3 SMBH to halo mass ratio

We now explore several further consequences. For the estimation of SMBH mass, it is usually assumed that quasar emission is isotropic, and that emission is at the Eddington rate, resulting in SMBHs powering the highest-redshift quasars having inferred masses (Fan et al. 2001b) of $\sim 10^9 M_\odot$. These estimates are consistent with dynamical estimates based on emission-line profiles (Willott, McLure & Jarvis 2003). We have therefore labelled the upper axis of the left-hand panel in Fig. 2 with the fraction of halo mass contributed by a $10^9 M_\odot$ black hole, allowing the curves in this panel to represent the a posteriori probability distributions for this fraction as well as M . We find that the full data set implies SMBHs contribute a fraction of about $10^{-2.9 \pm 0.2}$ ($M_{\text{bh}}/10^9 M_\odot$) and $\sim 10^{-2.6 \pm 0.2}$ ($M_{\text{bh}}/10^9 M_\odot$) of the halo mass for $\alpha = 3/2$ and 0, respectively. These fractions are larger than those found by Ferrarese (2002) for *local* $\sim 10^{12} M_\odot$ galaxies, which are $M_{\text{bh}}/M = 10^{-5.6}$, 10^{-5} and $10^{-4.2}$, respectively, under the assumptions of singular isothermal haloes, Navarro, Frenk & White (1997) (NFW) haloes and halo masses derived from galaxy–galaxy lensing (Seljak 2002). The difference between the inferred SMBH to halo mass ratio at high redshift is significantly larger than the scatter in the local estimate of the SMBH–halo mass relation of ~ 0.5 dex (Ferrarese 2002).

This result has two possible interpretations. First, the SMBHs are accreting at well above their Eddington rate and/or with high efficiency, so that the black hole mass has been overestimated (this disagrees with dynamical studies, Willott et al. 2003). Secondly, more agreeable interpretation is that SMBHs may contribute a larger fraction of the halo mass at higher redshifts. Indeed, this latter scenario

is independently supported by observations of quasar host galaxies at $z \sim 2$ which suggest black hole masses that are significantly larger with respect to their hosts than in the case of local galaxies (Croom et al. 2004).

2.4 Sensitivity to σ_8

Of the observable cosmological parameters, the relationship between B and M is most sensitive to σ_8 . To illustrate the extent of this dependence, we have repeated our analysis using values of $\sigma_8 = 0.76$ and 0.92 . (These values bound the 2σ range of the best-fitting constraints derived from *WMAP* plus large-scale structure and Ly α forest data Spergel et al. 2003.) We find that the constraints on the quasar host halo mass vary by a factor of ~ 4 within the 2σ range for σ_8 (see Fig. 3).

2.5 Marginalized distributions

One can also marginalize over systematic uncertainty in dP/dM due to α and σ_8 :

$$\frac{dP}{dM} \propto \int_0^{3/2} d\alpha \int_0^\infty d\sigma_8 \exp \left[\frac{-(\sigma_8 - 0.84)^2}{2(0.04)^2} \right] \frac{dP}{dM}(\alpha, \sigma_8), \quad (4)$$

where $(dP/dM)(\alpha, \sigma_8)$ was determined using equation (3), and we have used a flat prior probability for α in the range $0 \leq \alpha \leq 3/2$ combined with a Gaussian probability distribution for σ_8 . We find (left-hand panel of Fig. 4) a value of $M = 10^{11.7 \pm 0.3} M_\odot$, which is our best estimate for the halo mass of the high-redshift galaxies that host the quasars under the null hypothesis of $\gamma = 0$. Assuming a $10^9 M_\odot$ central black hole, corresponding to accretion at the Eddington limit (Willott et al. 2003), this corresponds to a black hole to halo mass ratio of $10^{-2.7 \pm 0.3}$, which is inconsistent with local estimates (Ferrarese 2002; $\sim 10^{-5}$ assuming an NFW profile) at greater than 7σ . If luminous quasars shine near their Eddington rate over a range of redshifts, we therefore conclude that the SMBH to halo mass ratio must increase with redshift.

2.6 Mass estimates assuming an evolving SMBH to halo mass ratio

In evaluating the derivative B , we have thus far assumed a luminosity M_{1450} to be associated with a fixed halo mass ($\gamma = 0$). However, if the halo mass M housing quasars of luminosity M_{1450} varies with redshift, then the evaluation of B must include the extra term in

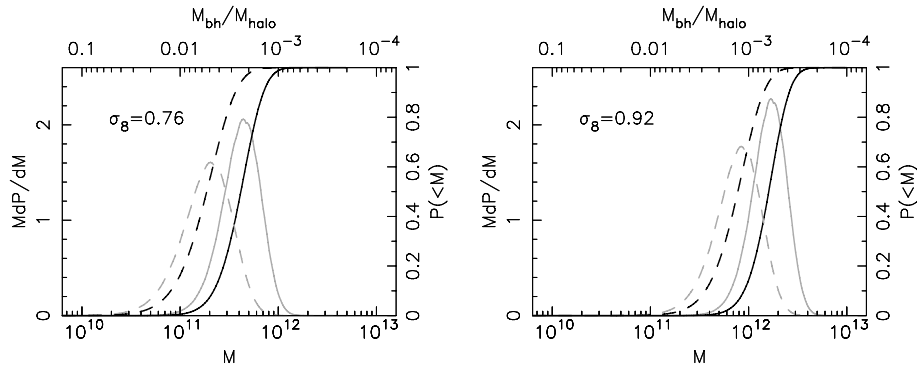


Figure 3. Constraints on the mass of dark matter haloes which host quasars. The a posteriori differential (grey lines) and cumulative (dark lines) probability distributions for M obtained using values of $\sigma_8 = 0.76$ and 0.92 . These correspond to the 2σ range for σ_8 determined from *WMAP* (Spergel et al. 2003). The solid and dashed curves in these panels correspond to $\alpha = 3/2$ and 0 . In each panel, the upper axis shows the corresponding values for the fraction of halo mass contributed by a $10^9 M_\odot$ black hole.

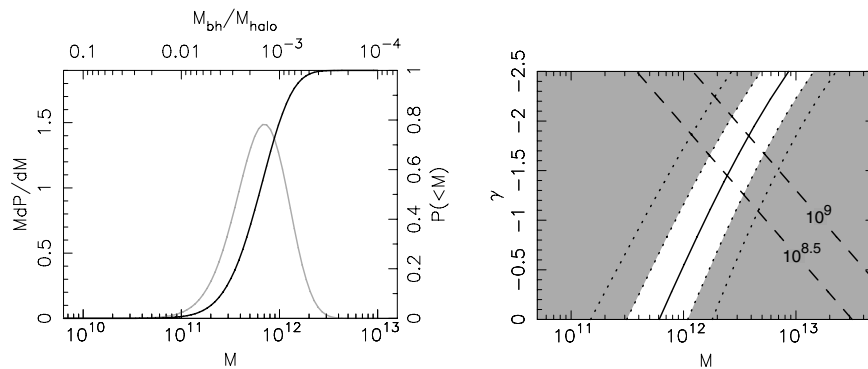


Figure 4. Constraints on the mass of dark matter haloes which host quasars. Left-hand panel: a posteriori probability distributions for M that have been marginalized over α and σ_8 (see equation 4). The upper axis shows the corresponding values for the fraction of halo mass contributed by a $10^9 M_\odot$ black hole. Right-hand panel: the 2.5, 16, 50, 84 and 97.5 percentiles of the cumulative marginalized probability for mass M as a function of γ . The grey regions represent masses outside the 1σ range for each γ . For comparison, we show curves (dashed lines) representing quasar host halo mass at high redshift derived assuming the local black hole halo mass ratio (Ferrarese 2002; for a $10^{8.5}$ and $10^9 M_\odot$ SMBH, and the NFW profile) plus an evolution of this ratio with redshift that is proportional to $(1+z)^{-\gamma}$.

equation (1) of the form $[\gamma M(z)/(1+z)][d \log_{10} N(>M, z)/dM]$ [where we have assumed that the halo mass varies as $M \propto (1+z)^\gamma$ at fixed luminosity M_{1450}]. In the right-hand panel of Fig. 4, we show the 2.5, 16, 50, 84 and 97.5 percentiles of the cumulative marginalized distribution (equation 4) for the halo mass as a function of γ . The grey regions represent the masses outside the 1σ range for each γ . Smaller values of γ lead to larger estimates of the mass (note that the y -axis is reversed with γ decreasing from bottom to top). If the evolution of halo mass M housing a fixed black hole mass follows $M \propto (1+z)^\gamma$ between the local and high-redshift Universe, then we can estimate M at high redshift as a function of γ , by extrapolating the local relation (Ferrarese 2002) between the halo mass and the black hole mass. The resulting curves (taking the case of an NFW profile) are plotted for black hole masses of $10^{8.5}$ and $10^9 M_\odot$ (dashed lines from left to right). By comparing the two constraints, we find $\gamma \sim -(1.5-2)$, leading to estimates of halo mass that are $\sim 3-6$ times larger than our evolution-free ($\gamma = 0$) estimate. Note that these larger masses do not weaken our result that SMBHs comprised a larger fraction of galaxy mass at high redshift, as this behaviour is explicit when $\gamma < 0$. Interestingly, values of $\gamma < 0$ follow naturally from models where SMBH growth is self limiting through feedback on galactic gas (e.g. Haehnelt et al. 1998; Wyithe & Loeb 2003).

We see from Fig. 4 that if the evolution of the ratio between the SMBH and the halo mass (or more correctly, the ratio between the quasar luminosity and the halo mass) can be described as a power law in redshift, then an extrapolation from local observations combined with our evolution analysis implies a value of $\gamma \sim -3/2$. In the left-hand panel of Fig. 5, we plot the differential and cumulative probability distributions for M assuming $\gamma = -3/2$. As mentioned in the previous paragraph, we find larger masses than that were derived in Fig. 2 under the assumption of non-evolving ratio; we get $M = 10^{12.5 \pm 0.2}$ ($\alpha = 3/2$) and $10^{12.3 \pm 0.2} M_\odot$ ($\alpha = 0$).

3 QUASAR LIFETIME

If a fraction ϵ of dark matter haloes contains SMBHs, then the total lifetime of the quasar can be estimated (Haيمان & Hui 2001; Martini & Weinberg 2001) by dividing the quasar number density $\Psi(M_{1450} < -26.7, z)$ by ϵ times the number density $N(>M)$ of haloes larger than M , and then multiplying by the Hubble time (for $t_q < H^{-1}$). The a posteriori probability for the product ϵt_q is

$$\frac{dP}{d(\epsilon t_q)} \propto \left[\frac{d}{dM} \int d\Psi \frac{dP}{d\Psi} \epsilon t_q(\Psi, M) \right]^{-1} \frac{dB}{dM} \Big|_{B=B_{\text{obs}}} \frac{dP}{dB_{\text{obs}}}, \quad (5)$$

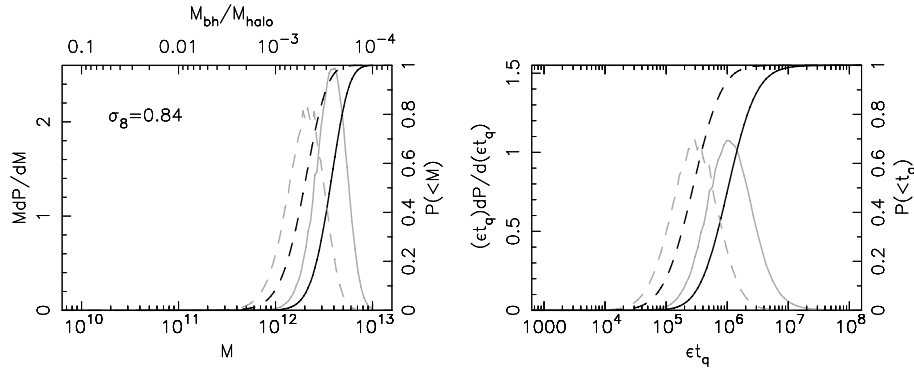


Figure 5. Constraints on the mass of the halo that hosts a high-redshift quasar. Left-hand panel: the a posteriori differential (grey lines) and cumulative (dark lines) probability distributions for M (solid lines $\alpha = 3/2$, dashed lines $\alpha = 0$; $\gamma = -1.5$). The upper axis shows the corresponding values for fraction of halo mass contributed by a $10^9 M_{\odot}$ black hole. Right-hand panel: the corresponding differential (grey lines) and cumulative (dark lines) probability distributions for ϵt_q . All curves in this figure were evaluated for $\sigma_8 = 0.84$.

where $dP/d\Psi$ is the observed Gaussian probability for Ψ . Under the assumption of a SMBH to halo mass ratio that does not evolve with redshift (see Fig. 2, right-hand panel), we find lifetimes of $10^{4.8 \pm 0.3} \epsilon^{-1}$ and $10^{4.3 \pm 0.4} \epsilon^{-1}$ yr, respectively, for $\alpha = 3/2$ and 0, in a cosmology where $\sigma_8 = 0.84$ (note that any evolution of ϵ with redshift is degenerate with that of t_q and is therefore implicit in the value of α). In addition (not shown), we have computed distributions for ϵt_q corresponding to $\sigma_8 = 0.76$ and 0.92. We find constraints that vary by a factor of 2 relative to the case of $\sigma_8 = 0.84$. These results imply that if all dark matter haloes contained SMBHs at high redshift ($\epsilon = 1$) then the preferred quasar lifetime of 10^4 – 10^5 yr is significantly shorter than both the Salpeter time [about $4 \times 10^7 (\epsilon_{\text{eff}}/0.1)\eta^{-1}$ yr] for accretion at the maximal rate ($\eta = 1$) with $\epsilon_{\text{eff}} = 10$ per cent efficiency of conversion from mass to energy as well as estimates of the quasar lifetime at lower redshifts [10^6 – 10^8 yr; see Martini (2003) for a summary]. The small value of ϵt_q might therefore indicate that not all dark matter haloes at high redshift contain SMBHs, in contrast to the situation locally (Kormendy & Richstone 1995). Indeed, if the high-redshift quasar lifetime were 10^6 – 10^8 yr, as seems to be the case (Yu & Tremaine 2002) at $z \sim 2$, this would imply that only 1 in 10 – 10^3 dark matter haloes at $z > 4$ contained a SMBH. Alternatively, there could be a larger number of obscured quasars at high redshift, giving the impression of a smaller quasar lifetime.

On the other hand, we have suggested that a situation, where the SMBH to halo mass ratio does not evolve with redshift, will be inconsistent with local observations. As a result, it should not be surprising that the lifetime derived when $\gamma = 0$ is inconsistent with other observations. In Section 2.6, we derived results for the halo mass under the assumption that the SMBH to halo mass ratio evolves as a power law in redshift [$\propto (1+z)^{-\gamma}$] and found that larger masses of $M \sim 10^{12.4 \pm 0.3} M_{\odot}$ are obtained for $\gamma = -1.5$. We have also derived the a posteriori probability distribution for quasar lifetime in this case (right-hand panel of Fig. 5), and found that the larger halo mass leads to a longer inferred lifetime. In the case of a quasar lifetime that is constant with redshift ($\alpha = 3/2$), we find $t_q = 10^{5.9 \pm 0.4} \epsilon^{-1}$ yr. For occupation fractions of unity ($\epsilon = 1$), this lifetime is consistent with the lifetime inferred at lower redshift. In scenarios where feedback limits SMBH growth, the quasar lifetime is thought to be proportional to the host's dynamical time ($\alpha = 0$). In this case, we find $t_q = 10^{5.5 \pm 0.5} \epsilon^{-1}$ yr, which again compares favourably with the lifetime inferred at $z \sim 2$ when the factor $(1+z)^{3/2}$ in the extrapolation from $z \sim 2$ to 4.3 is accounted for.

Before leaving this section, we comment on the possibility that ϵ increases towards low redshift (since $\epsilon \sim 1$ at $z = 0$, it cannot decrease towards low redshift). As mentioned in Section 2, the evolution of ϵ is degenerate with t_q . Evolution of ϵ may therefore be described by a value of α that is smaller than the $\alpha = 0$ or $3/2$ that describe the evolution of lifetime. The adoption of smaller values of α leads to smaller estimates of mass, and hence strengthen the prime result of this paper, that quasar hosts were smaller in the past than today.

4 THE VARIANCE OF DENSITY FLUCTUATIONS CORRESPONDING TO HIGH-REDSHIFT QUASAR HOSTS

An alternative way of studying the hosts of the high-redshift quasars is to compare the evolution of their density with the evolution of the density of haloes that correspond to scales with a fixed variance in the linearly extrapolated power spectrum. In Fig. 6, we show curves of density [$\tau N(>M(\sigma), z)$] against redshift for values of variance $\sigma = 2, 2.5$ and 3. Since we are interested in the *deviation* of the observed results from the theoretical curves for a constant σ , we have normalized both the theoretical curves (from Press–Schechter) and the data to unity at an intermediate redshift $z = 4.8$, and thus express the evolution in terms of a dimensionless density parameter [$\Omega(z)/\Omega(4.8)$]. The left- and right-hand panels correspond to values of $\alpha = 3/2$ and 0, respectively. We find that the values of $\sigma = 2$ –3 bracket the range of evolution, implying that for a linearly extrapolated critical overdensity of $\delta_c \sim 1.69(1+z)$, the high-redshift quasar dark matter host galaxies formed from $\sim 3\sigma$ to 4.5σ density fluctuations. The rareness of these fluctuations is consistent with the large masses (well in excess of the non-linear mass-scale) which were inferred in Section 2.6.

5 THE LINEAR OVERDENSITY FOR QUASAR HOSTS

When calculating the Press–Schechter mass function, we have so far adopted the conventional value for the linear overdensity at halo virialization of $\delta_c = 1.69$, which is appropriate for a spherical collapse at the time when shells evolve to zero radius. This value of δ_c , which corresponds to a non-linear overdensity of about 178, agrees with results from N -body simulations (Jenkins et al. 2001). However, in general, non-spherical top-hat models virialize at a time when the

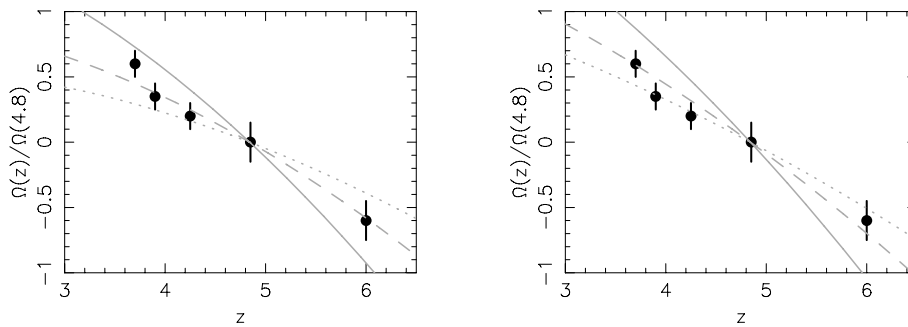


Figure 6. The evolution of density with redshift for different values of linear variance σ corresponding to haloes that host high-redshift quasars. The curves correspond to $\sigma = 2$ (solid line), $\sigma = 2.5$ (dashed line) and $\sigma = 3$ (dotted line). Both the model and quasar densities have been normalized to unity at $z = 4.8$. Left-hand panel: curves for $\alpha = 3/2$. Right-hand panel: curves for $\alpha = 0$.

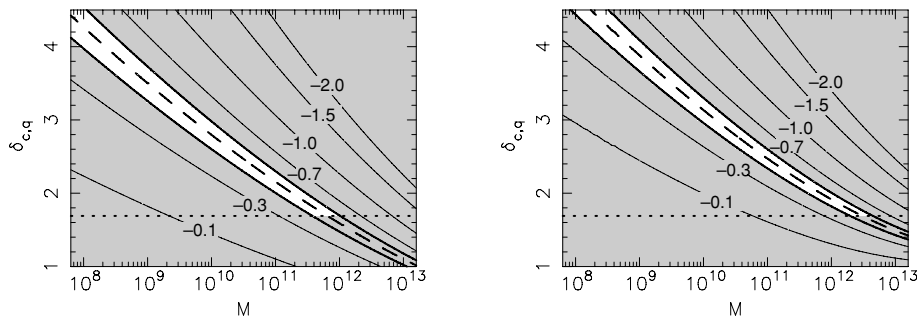


Figure 7. Contours of the exponential slope B as a function of the linear overdensity for quasars $\delta_{c,q}$ and host halo mass M (we assumed $\alpha = 3/2$). The shaded regions are excluded by the requirement that $\delta_{c,q} > 1.69$, and by the limits on B_{obs} derived from the redshift evolution in the quasar luminosity function. The dashed line shows the most likely value for the slope, and the dotted line corresponds to $\delta_{c,q} = 1.69$. Left-hand panel: curves for $\gamma = 0$. Right-hand panel: curves for $\gamma = -1.5$. All curves in this figure were evaluated for $\sigma_8 = 0.84$.

linear overdensity reaches a value greater (Engineer, Kanekar & Padmanabhan 2000) than $\delta_c = 1.69$.

As we showed in Section 4, luminous quasars are rare systems forming from greater than 3σ fluctuations. It is therefore possible that they form only in hosts of unusual overdensity. In Fig. 7, we have plotted contours of B as a function of δ_c and M . [For the case of $\alpha = 3/2$ and $\sigma_8 = 0.84$, and assuming $\gamma = 0$ (left-hand panel) and $\gamma = -3/2$ (right-hand panel).] The shaded grey regions show the excluded values of $\delta_c < 1.69$ and B (68 per cent range). The most likely value of the variance is plotted as a thick dashed line. We see that δ_c cannot be too different from 1.69, or else the host dark matter haloes would be unacceptably small. This indicates that collapse to an unusually overdense halo is not taking place in haloes that host SMBH formation and quasar activity. An absolute upper limit on δ_c can be obtained by noting that if the mass of the SMBH is $10^9 M_\odot$, then host masses must be larger than about $10^{10} M_\odot$. In this case, values of $\delta_c \gtrsim 3$ are not allowed. If the SMBH were restricted to contain less than 10 per cent of the gas component, then $\delta_c \lesssim 2$.

6 DISCUSSION

In this paper, we have estimated the mass of high-redshift quasar host dark matter haloes by comparing the rate of quasar evolution with the Press–Schechter mass function. We have found in the case of the null hypothesis, where the SMBH to halo mass ratio does not change with redshift, that the implied halo mass is $M = 10^{11.7 \pm 0.3} M_\odot$. This mass is significantly smaller than the mass of local haloes that house a $10^9 M_\odot$ SMBH, the mass believed to be powering the SDSS quasars. Indeed, our results rule out the null hypothesis at a

significance greater than 5σ . We therefore conclude that the SMBH to halo mass ratio must increase towards higher redshift, i.e. SMBHs contained a larger fraction of the host galaxy mass at earlier times.

Having demonstrated that SMBHs at high redshift must have contained a larger fraction of the host mass than SMBHs observed today, we allowed the SMBH to halo mass ratio to vary with redshift. In this case, it is possible to achieve consistency between observations of high-redshift quasars and local SMBH masses. We find that these combined constraints imply high-redshift quasar host halo masses of $M = 10^{12.4 \pm 0.3}$, with a SMBH to halo mass ratio that varies with redshift approximately as $(1+z)^{3/2}$.

A scenario, where SMBHs formed at high redshift contain a greater fraction of the host galaxies mass, is consistent with models of SMBH evolution in which SMBH growth is limited by feedback during the quasar phase (e.g. Haehnelt et al. 1998; Silk & Rees 1998; Wyithe & Loeb 2003). These models predict a relation between SMBH mass and the characteristic velocity of the host which is redshift independent. As a result, feedback-regulated growth of SMBHs leads naturally to a ratio of SMBH to halo mass that increases with redshift. Our results therefore support feedback-regulated schemes, where SMBH growth is dominated by accretion during the luminous quasar phase.

Upon completion, the SDSS will have identified much larger numbers of high-redshift quasars than are currently published. The more accurate luminosity functions which will be available should then allow a similar and more precise analysis using the model-independent technique introduced in this work. Such an analysis may allow the variation of host mass with redshift to be determined directly for the high-redshift quasars.

ACKNOWLEDGMENTS

The work of JSBW was supported by the Australian Research Council. This work was initiated when one of the authors (TP) was visiting the School of Physics, University of Melbourne, under the Miegunah Distinguished Fellowship.

REFERENCES

- Bardeen J. M., Bond J. R., Kaiser N., Szalay A. S., 1986, *AJ*, 304, 15
 Barkana R., Loeb A., 2003, *Nat*, 421, 341
 Bertoldi F. et al., 2003, *A&A*, 409, 47
 Croom S. M., Schade D., Boyle B. J., Shanks T., Miller L., Smith R. J., 2004, *AJ*, 606, 126
 Croom S. M. et al., 2005, *MNRAS*, 356, 415
 Efstathiou G., Rees M. J., 1998, *MNRAS*, 230, 5
 Engineer S., Kanekar N., Padmanabhan T., 2000, *MNRAS*, 314, 279
 Fan X. et al., 2001a, *AJ*, 121, 54
 Fan X. et al., 2001b, *AJ*, 122, 2833
 Fan X. et al., 2003, *AJ*, 125, 1649
 Fan X. et al., 2004, *AJ*, 128, 515
 Ferrarese L., 2002, *ApJ*, 578, 90
 Haehnelt M. G., Natarajan P., Rees M. J., 1998, *MNRAS*, 300, 817
 Haiman Z., Hui L., 2001, *AJ*, 547, 27
 Haiman Z., Loeb A., 1998, *ApJ*, 503, 505
 Jenkins A., Frenk C. S., White S. D. M., Colberg J. M., Cole S., Evrard A. E., Couchman H. M. P., Yoshida N., 2001, *MNRAS*, 321, 372
 Kauffmann G., Haehnelt M. G., 2000, *MNRAS*, 311, 576
 Kormendy J., Richstone D., 1995, *ARA&A*, 33, 581
 Martini P., 2003, in Ho L. C., ed., *Carnegie Obs. Astrophys. Ser. Vol. 1, Coevolution of Black Holes and Galaxies*. Cambridge Univ. Press, Cambridge (astro-ph/0304009)
 Martini P., Weinberg D. H., 2001, *AJ*, 547, 12
 Merritt D., Ferrarese L., 2001, *ApJ*, 547, 140
 Navarro J. F., Frenk C. S., White S. D. M., 1997, *AJ*, 490, 493
 Press W. H., Schechter P., 1974, *AJ*, 187, 425
 Scannapieco E., Oh S. P., 2004, *ApJ*, 608, 62
 Seljak U., 2002, *MNRAS*, 334, 797
 Sheth R., Torman G., 2002, *MNRAS*, 321, 61
 Silk J., Rees M. J., 1998, *A&A*, 331, L1
 Spergel D. N. et al., 2003, *ApJS*, 148, 175
 Tremaine S. et al., 2002, *ApJ*, 574, 740
 Volonteri M., Haardt F., Madau P., 2003, *AJ*, 582, 559
 Willott C. J., McLure R. J., Jarvis M. J., 2003, *AJ*, 587, L15
 Wyithe J. S. B., Loeb A., 2003, *AJ*, 595, 614
 Yu Q., Tremaine S., 2002, *MNRAS*, 335, 965

This paper has been typeset from a $\text{T}_{\text{E}}\text{X}/\text{L}_{\text{A}}\text{T}_{\text{E}}\text{X}$ file prepared by the author.